Available online at www.sciencedirect.com
ScienceDirect
Journal of Power Sources 164 (2007) 857–861
JOURNAL OF POWER SOURCES
www.elsevier.com/locate/jpowsour

Short communication

Synthesis and characterization of Nd doped $LiMn_2O_4$ cathode for Li-ion rechargeable batteries

Rahul Singhal [a], Suprem R. Das [b], Maharaj S. Tomar [a], Osbert Ovideo [a], Santander Nieto [c], Ricardo E. Melgarejo [a], Ram S. Katiyar [b,*]

[a] *Department of Physics, University of Puerto Rico, Mayaguez, PR 00680-9016, USA*
[b] *Department of Physics, University of Puerto Rico, San Juan, PR 00931-3343, USA*
[c] *School of Science and Technology, University of Turabo, Gurabo, PR 00778-3030, USA*

Received 10 August 2006; received in revised form 19 August 2006; accepted 16 September 2006
Available online 4 December 2006

Abstract

Spinel powders of $LiMn_{1.99}Nd_{0.01}O_4$ have been synthesized by chemical synthesis route to prepare cathodes for Li-ion coin cells. The structural and electrochemical properties of these cathodes were investigated using X-ray diffraction (XRD), scanning electron microscopy (SEM), Raman spectroscopy, cyclic voltammetry, and charge-discharge studies. The cyclic voltammetry of the cathodes revealed the reversible nature of Li-ion intercalation and deintercalation in the electrochemical cell. The charge-discharge characteristics for $LiMn_{1.99}Nd_{0.01}O_4$ cathode materials were obtained in 3.4–4.3 V voltage range and the initial discharge capacity of this material were found to be about 149 mAh g^{-1}. The coin cells were tested for up to 25 charge-discharge cycles. The results show that by doping with small concentration of rare-earth element Nd, the capacity fading is considerably reduced as compared to the pure $LiMn_2O_4$ cathodes, making it suitable for Li-ion battery applications.

Keywords: Li-ion battery; $LiMn_2O_4$; Cyclic voltammetry; Spinel cathode; Discharge capacity

1. Introduction

During the past decade, a number of efforts were made by researchers towards the development of high performance rechargeable Li-ion batteries with high specific capacity, long cycleability, and calendar life [1–7]. The discovery of new intercalation materials through different crystal chemistries and improved solid-state engineering should lead to the emerging superior Li-ion battery technologies. The commercial Li-ion batteries based on $LiCoO_2$ cathode materials, which have several drawbacks, e.g., high cost and toxicity of cobalt. Many efforts are being made to make lithium manganate ($LiMn_2O_4$) (LMO) spinel cathode viable as an alternate to $LiCoO_2$ because of its economical and non-toxic nature [8–14]. However, pure $LiMn_2O_4$ has several drawbacks which prevent it from commercialization in Li-ion batteries, e.g., it suffers from the capacity fading and the structural instability, especially at 3 V range operation and at elevated temperatures. This capacity loss is reported to be due to several reasons [15,16] such as (i) the phase transition from cubic to tetragonal phase upon 3 V cycling; (ii) the micro-crack formation on the surface of the cathode material after electrochemical cycling; (iii) the formation of a surface dead layer (SEI layer) on the surface of the electrodes after electrochemical cycling, and (iv) the formation of oxygen vacancies due to the dissolution of manganese in the electrolyte. $LiMn_2O_4$ cathode, even in the 4 V range, shows poor cycleability as reported by several workers [17–19]. However, the phase transformations and the volume changes in spinel $LiMn_2O_4$ are mostly reported to affect the capacity. Ahn and Song [20] prepared $LiMn_2O_4$ by solid-state reaction at various temperatures between 650 °C to 900 °C. The initial discharge capacities of all the samples were found to be less then 100 mAh g^{-1}. They found that the sample annealed at 750 °C for 48 h shows the highest discharge capacity and best cycling performance due to its crystallinity and large grain size. He et al. [21] prepared spherical $LiMn_2O_4$ by controlled crystallization method. The initial discharge capacity of the synthesized materials was found to be about 125 mAh g^{-1} with capacity retention of 92.4% after 100

* Corresponding author. Tel.: +1 787 751 4210; fax: +1 787 764 2571.
E-mail address: rkatiyar@speclab.upr.edu (R.S. Katiyar).

0378-7753/$ – see front matter © 2006 Published by Elsevier B.V.
doi:10.1016/j.jpowsour.2006.09.098

cycles. Lee and Yoshino [22] reported that the spinel structure becomes more tolerant to repeated charging and discharging, by doping of Al in the Mn site. They found that $LiMn_2O_4$ exhibits typical capacity loss in 3–4 V ranges. In the 3 V range the capacity retention was ~60% after 50 cycles while in the 4 V range it was found to be about 70% of its initial value. Furthermore, they reported that the Al doped LMO ($LiAl_{0.1}Mn_{1.9}O_4$) exhibited excellent capacity retention (96%) in the 4 V range, while in the 3 V range it decreased drastically to 40% of its initial value after 50 cycles. Nieto et al. [23] synthesized $LiMn_2O_4$ and $Li_{1.2}Al_{0.05}Mn_{1.95}O_4$ by acetate based chemical solution route. They found that a small amount of codoping with Al and Li (by replacing Mn in the octahedral 16d site) reduced the discharge capacity by 10% as compared to pure $LiMn_2O_4$ but the cycleability improved dramatically. Kannan and Manthiram [24] have synthesized layered $LiNi_{0.85}Co_{0.15}O_2$ and $LiNi_{0.85}Co_{0.12}Al_{0.03}O_2$ oxides by a gel method and a hydroxide precursor method. They found that the $LiNi_{0.85}Co_{0.12}Al_{0.03}O_2$ oxide prepared by the hydroxide precursor route exhibits a reversible capacity of around 170 mAh g^{-1} with improved cyclability. Molendra et al. [25] reported that the phase transition in manganese spinel can be suppressed by Cr doping. They also reported that $Li_yCr_xMn_{2-x}O_4$ cathode material could be used for 5 V battery, where 5 V potential corresponds to the oxidation of Cr^{+3} into Cr^{+4}. Often surface morphology, particle size, microstructure and morphology of the cathode materials also play important roles in improving the electrochemical properties [26]. Bao et al. [26] reported that $LiCr_{0.1}Mn_{1.9}O_{3.95}F_{0.05}$, prepared by sol–gel method have slightly larger and predominantly cubic spinel structure as compared to that of $LiCr_{0.1}Mn_{1.9}O_4$. The discharge capacity of $LiCr_{0.1}Mn_{1.9}O_{3.95}F_{0.05}$ was found to be ~130.6 mAh g^{-1} and it reduced to 116.6 mAh g^{-1} after 30 cycles.

Substitutions of rare-earth elements like La, Nd etc. often play major role in controlling the cationic disorders and hence structural and electrical properties in most perovskite structures [27,28]. In the hope that such substitutions might affect the electrochemical properties of cathode materials, synthesized rare-earth element Nd doped $LiMn_2O_4$ ($LiMn_{1.99}Nd_{0.01}O_4$) cathode, replacing a very small amount of Mn by Nd and we studied its structural and electrochemical behavior. This material has clearly demonstrated a good improvement in the capacity and cycleability in a Li-ion cell.

2. Experimental

99.9% pure grade lithium acetate [$LiOOCCH_3{\cdot}2H_2O$], Manganese (II) acetate [$Mn(CH_3COO)_2{\cdot}4H_2O$] and nickel acetate [$Ni(CH_3COO)_2{\cdot}4H_2O$] (Alfa Aesar) were used as precursor materials. Neodymium acetate hydrate [$Nd(OOCCH_3)_3{\cdot}XH_2O$] was used for Nd doping in lithium manganate powder. As the rare-earth elements (La, Nd) doping were expected to stabilize the structure [27,28] and hence electrochemical properties, we do not yet know the effect of higher concentration of Nd doping, and the work has to be extended, but we intended to start with a lower concentration of Nd doping (1%) in $LiMn_2O_4$ cathode material. The stoichiometric ratios of these metallic salts were dissolved separately in 2-ethylhexanoic acid at 50 °C, followed by continuous stirring for about 1 h. Afterwards, all solutions were mixed and heated at 50 °C for 4 h, followed by continuous stirring. The resulting solution was dried overnight at about 100 °C to get $LiMn_{1.99}Nd_{0.01}O_4$ in the powder form. The obtained powders were fired at 400 °C for 4 h in air for complete organic removal. The powders after organic removal were calcined at various temperatures from 700 °C to 900 °C with an increment of 50 °C. The phase formation behavior of the calcined powder was characterized by XRD (Siemens D5000 powder diffractometer), using Cu Kα radiation (operated at 45 kV and 30 mA) and at a scan rate of 3° min^{-1}. The cathode was prepared by mixing above active material, carbon black and polyvinylidene fluoride (PVDF) in a weight ratio of (80:10:10) and emulsified in *n*-methyl-2 pyrolidon. The resulting paste was spread on aluminum foil and dried overnight at about 100 °C. The coin cell was prepared in an Ar atmosphere inside a glove box (MBraun, USA) using Li metal foil as anode and electrolyte consisting of 1 M $LiPF_6$, dissolved in ethylene carbonate and diethyl carbonate (1:2 volume ratio). The working electrode and Li metal foil were separated using Cellgard 2400 membrane. The cyclic voltammetric studies were carried out at room using PC 4.750 potentiostat/galvanostat controller electronics and PHE 200 electrochemical software (Gamry Instruments Inc.). The charge-discharge measurements were carried out at room temperature and at a current density of 0.2 mA cm^{-2} in 3.5–4.3 V range.

3. Results and discussions

Fig. 1 shows XRD powder patterns of $LiMn_{1.99}Nd_{0.01}O_4$ (Nd–LMO), calcined at 850 °C for 14 h. All of the peaks in the XRD pattern correspond to the cubic spinel structure. The phase purity of Nd–LMO was confirmed from the absence of any secondary peak in the spectra. The crystallinity of the polycrystalline Nd–LMO was determined from the peak intensities

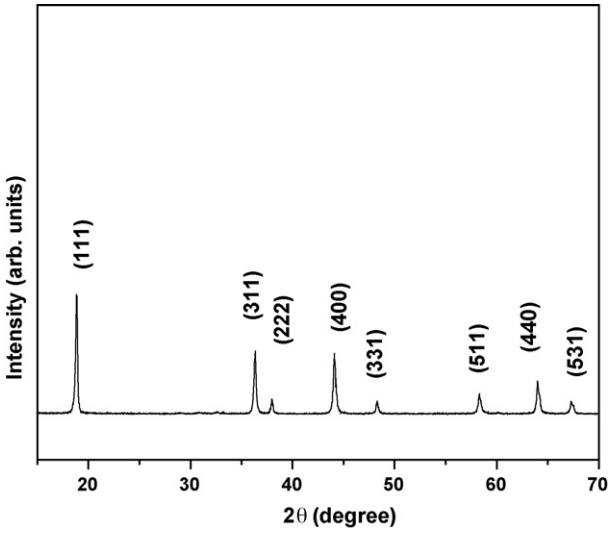

Fig. 1. XRD pattern of as prepared $LiMn_{1.99}Nd_{0.1}O_4$ cathode material, calcined at 850 °C for 14 h.

and peak widths of the diffraction lines. The analysis of the diffraction data was performed by Peakfit software using Pearson VII amplitude function curve fitting. Comparing the results of pure $LiMn_2O_4$ [13,20,21] with the dope ones, it is evident that the spinel structure did not change due to small doping of neodymium in the octahedral site (16d) in the crystal lattice. The lattice parameter for $LiMn_{1.99}Nd_{0.01}O_4$ was determined from the XRD patterns and it was found to be about 8.2539 Å, which is very similar to that of the pure $LiMn_2O_4$.

Fig. 2 shows the cyclic voltammogram of the coin cells containing Nd–LMO as cathode material. All measurements were taken at room temperature at a scan rate of 0.1 mV s^{-1} and in voltage range of 3.5–4.5 V Li/Li^+. The two cathodic peaks during charging at 3.84 V and 4.015 V correspond to two-step Li^+ de-intercalation from the cathode and two anodic peaks at 4.146 V and 4.284 V correspond to Li^+ intercalation into the cathode. The distinct separation of the peaks (of magnitude $\Delta E_p \sim 0.16$ V) and the their symmetrical nature during both oxidation and reduction revealed the reversible/quasireversible nature of Li^+-transport in the electrochemical cell between $LiMn_2O_4$ and λ-MnO_2 structures.

Fig. 3 shows the charge-discharge characteristics of Nd–LMO, carried out at room temperature in 3.5–4.3 V range, at a current density of 0.2 mA cm^{-2}. It can be seen that the initial charge and discharge capacities of Nd–LMO cathode material were about 166 mAh g^{-1} and 149 mAh g^{-1}, respectively. The irreversibility of about 10% in first cycle may be due to the formation of solid electrolyte interface (SEI) layer onto the spinel $LiMn_{1.99}Nd_{0.01}O_4$, as explained earlier by Zhang et al. [29]. After 25 cycles, the discharge capacity was found to be about 132 mAh g^{-1}. Fig. 4 shows the cycleability of the Nd–LMO electrode for 25 charge-discharge cycles. It can be seen from the figure that after 25 cycles the initial discharge capacity retention is about 91%. This improvement in the cycleability is believed to be due to the structural stability by Nd doping in $LiMn_2O_4$. Table 1 shows the comparison of the discharge capacities of our $LiMn_{1.99}Nd_{0.01}O_4$ with pure $LiMn_2O_4$, reported by various researchers.

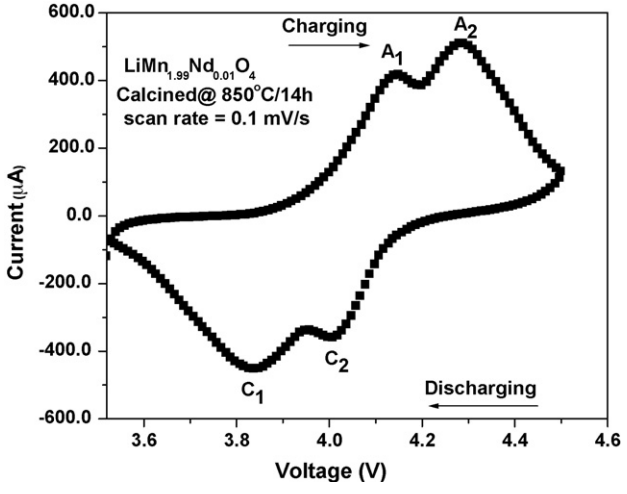

Fig. 2. Cyclic voltammetry of $LiMn_{1.99}Nd_{0.1}O_4$/(EC + DMC)/Li coin cell in 3.5–4.5 V range at a scan rate of 0.1 mV s^{-1}.

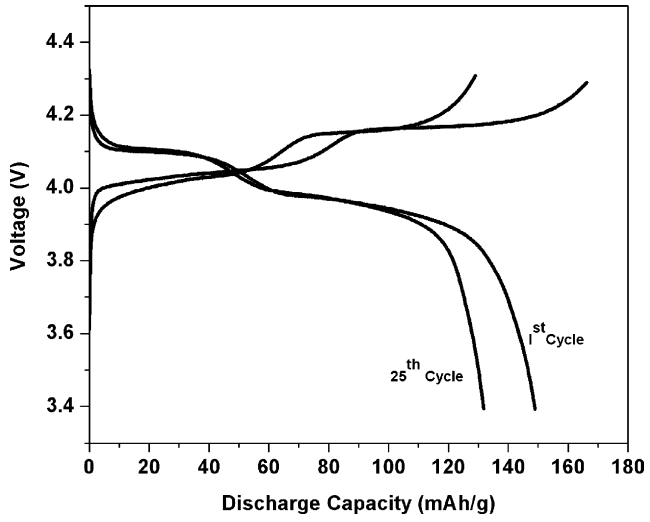

Fig. 3. Charge-discharge characteristics of 1st and 25th cycle of $LiMn_{1.99}Nd_{0.1}O_4$ coin cell at room temperature and 0.2 mA cm^{-2} between 3.5 V and 4.3 V.

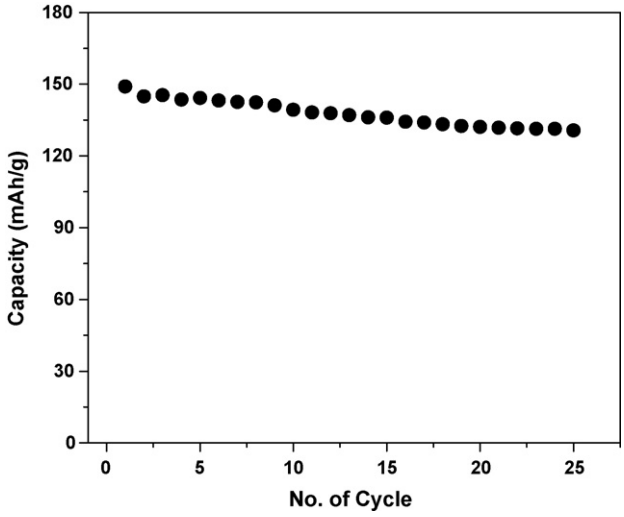

Fig. 4. The discharge capacity vs. number of cycle of $LiMn_{1.99}Nd_{0.1}O_4$/(EC + DMC)/Li coin cells.

In most cases the microstructure and surface morphology are important factors in deciding the appropriate diffusion pathway that improves the Li^+ intercalation kinetics. Larger grain size involves slow diffusion coefficient of Li^+ ion in the host whereas the smaller grains produce higher diffusion coefficient, due to decrease in the diffusion distance. However, the scaling is not

Table 1
Comparison of discharge capacities of $LiMn_2O_4$ with $LiMn_{1.99}Nd_{0.01}O_4$ cathode materials

S. no.	Cathode material	Initial discharge capacity (mAh g^{-1})	Discharge capacity after 25 cycles	Reference
1	$LiMn_2O_4$	125	115	[21]
2	$LiMn_2O_4$	118	105	[32]
3	$LiMn_2O_4$	120	15	[28]
4	$LiMn_{1.99}Nd_{0.01}O_4$	149	132	Present work

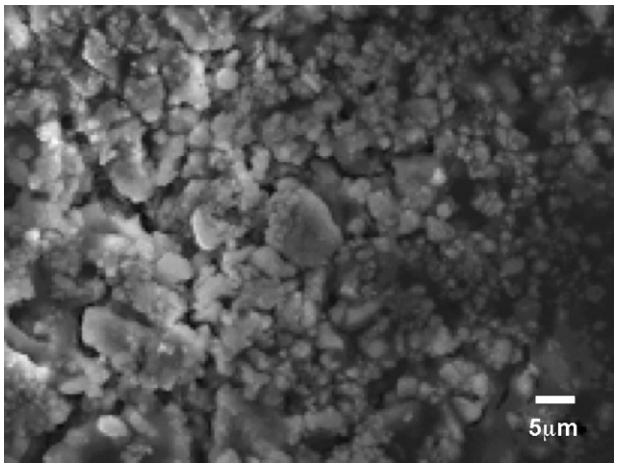

Fig. 5. SEM micrograph of $LiMn_{1.99}Nd_{0.1}O_4$ cathode before charge-discharge cycles.

so simple and linear as it appears and there are controversies in nanoscale region regarding the electrochemical performances of Li-ion batteries [30]. In case of our samples, the grains are in the micron scale and hence there is no ambiguity in the correlation. Figs. 5 and 6 show the scanning electron micrograph of Nd doped cathode materials before and after 25 charge-discharge cycles, respectively. It can be seen from the figure that the grain size

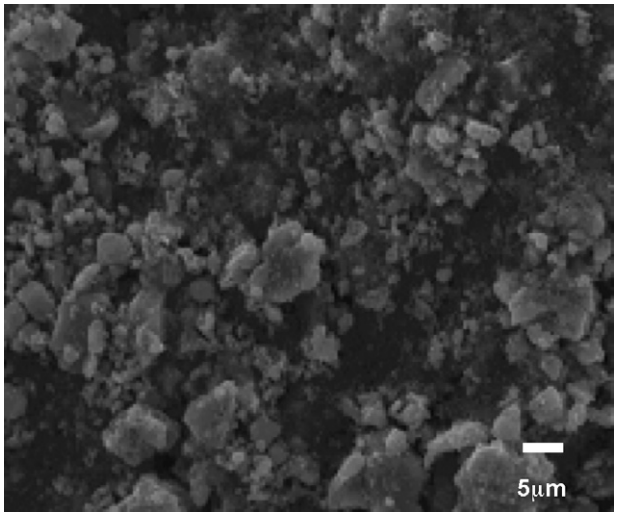

Fig. 6. SEM micrograph of $LiMn_{1.99}Nd_{0.1}O_4$ cathode after charge-discharge cycles.

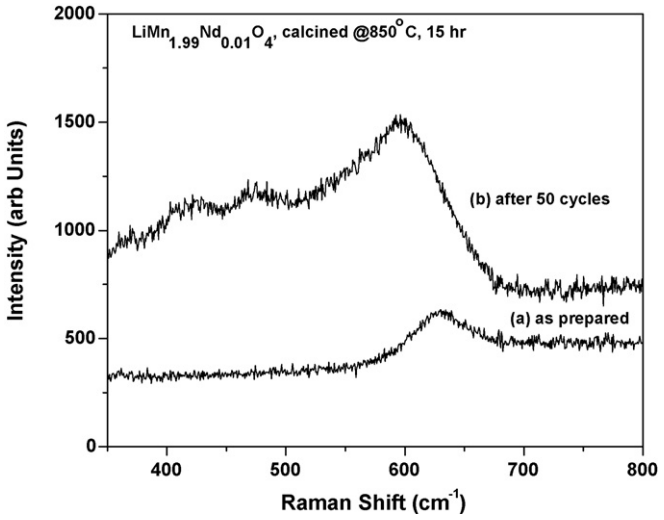

Fig. 7. Raman spectra of $LiMn_{1.99}Nd_{0.1}O_4$ cathode (a) before charge-discharge cycles; (b) after charge-discharge cycles.

is in the micron range. The average grain size from the SEM micrographs before and after 25 electrochemical cycling was found to be in 0.5–1.5 μm range.

Fig. 7 shows the Raman spectra of $LiMn_{1.99}Nd_{0.01}O_4$, before and after charge-discharge cycles measured using 514 nm excitations. Before charge-discharge cycles the most intense peak, A_{1g}, and the shoulder peak $T_{2g}^{(3)}$ appear at 628.13 cm^{-1} and 578.4 cm^{-1}, respectively, and all other Raman peaks of $LiMn_{1.99}Nd_{0.01}O_4$ were found to be extremely weak. A_{1g} mode is predominantly due to the oxide ion displacements in $Mn(Nd)O_6$ octahedra whereas $T_{2g}^{(3)}$ phonon is characterized by the large oxygen ion motions and very small Li displacements [31]. After charge-discharge cycles, many changes in the Raman spectra were noticed. The A_{1g} and $T_{2g}^{(3)}$ modes were shifted to lower wave number sides and also the FWHM were increased. The shift in wave number towards lower value may be due to the increased effective mass of Mn(Nd)–O bond because of larger atomic weight of Nd than Mn. The increase in FWHM is due to the disorder at the site of the oxygen octahedral. The appearance of the other Raman active modes at the peak positions of 426.77 cm^{-1} and 383.76 cm^{-1} were observed, which are assigned to $T_{2g}^{(2)}$ and E_g phonon modes, respectively. Further, these vibrations were assigned due to large oxygen ion motions. Table 2 shows the shifts in the various Raman modes after charge-discharge cycles of $LiMn_{1.99}Nd_{0.01}O_4$ cathode.

Table 2
Comparison of Raman peak position of $LiMn_{1.99}Nd_{0.01}O_4$ cathode material with pure $LiMn_2O_4$, before and after charge-discharge cycles

Phonon symmetry	$LiMn_2O_4$ (calculated positions in cm^{-1}) [32]	$LiMn_2O_4$ (observed positions in cm^{-1}) [32]	$LiMn_{1.99}Nd_{0.01}O_4$, peak position (cm^{-1}), before cycle	$LiMn_{1.99}Nd_{0.01}O_4$, peak position (cm^{-1}), after 25 cycles	Pek shift (cm^{-1})
A_{1g}	598	625	628.13	595.03	33.1
E_g	434	432	426.77	419.48	7.29
$T_{2g}^{(1)}$	354	365	383.76	380	3.76
$T_{2g}^{(2)}$	455	480	489.77	473.1	16.67
$T_{2g}^{(3)}$	597	590	579.04	578.4	0.64

4. Conclusions

We have synthesized phase pure $LiMn_{1.99}Nd_{0.01}O_4$ by chemical solution route. The XRD data showed the cubic spinel network (*Fd3m*). It is believed that the presence of Nd ion in the host LMO stabilizes the structure, leading to a more reversible electrochemical reaction. This is corroborated from the charge-discharge characteristics of the electrochemical cell. The initial discharge capacity of the $LiMn_{1.99}Nd_{0.01}O_4$ cathode material was found to be about 149 mAh g^{-1}, with the capacity retention of about 91% after 25 charge-discharge cycles. It can be seen that the severe capacity fading in $LiMn_2O_4$ cathode can be improved significantly by doping with small concentrations of rare-earth element such as Nd. The improvements were explained on the basis of the structural stabilities imposed by the rare-earth element. Structural analyses of the as prepared and cycled electrodes were investigated and from Raman spectroscopic results it has been concluded that the oxygen motions in the spinel framework play important roles in charge-discharge characteristics.

Acknowledgements

This research work was supported by the DoE-EPSCOR Grant (# DE-FG02-01ER45868). The support from the UPR Materials Characterization Center (MCC) is also acknowledged.

References

[1] J.M. Tarascon, F. Coowar, G. Amatucci, F.K. Shokoohi, D. Guyomard, J. Electrochem. Soc. 141 (1994) 1421.
[2] M. Broussely, P. Biensan, B. Simon, Electrochim. Acta 45 (1–2) (1999) 3.
[3] M.M. Thackeray, P.J. Johnson, L.A. de Piccioto, P.G. Bruce, J.B. Goodenough, Mater. Res. Bull. 19 (1984) 179.
[4] W.R. Liu, S.H. Wu, H.S. Sheu, J. Power Sources 146 (2005) 232.
[5] J.M. Tarascon, M. Armand, Nature 414 (2001) 359.
[6] S.S. Zhang, T.R. Jow, J. Power Sources 109 (2002) 172.
[7] Y. Gao, J.R. Dahn, J. Electrochem. Soc. 143 (1996) 100.
[8] H.J. Choi, K.M. Lee, G.H. Kim, J.G. Lee, J. Am. Ceram. Soc. 84 (1) (2001) 242.
[9] M.Y. Song, D.S. Ahn, H.R. Park, J. Power Sources 83 (1999) 57.
[10] K.A. Striebel, A. Rougier, C.R. Horne, R.P. Reade, E.J. Cairns, J. Electrochem. Soc. 146 (12) (1999) 4339.
[11] S.R. Das, S.B. Majumder, R.S. Katiyar, J. Power Sources 139 (2005) 261.
[12] C.R. Sides, N.L. Charles, J. Patrissi, B. Scorosati, C.R. Martin, Bull. Mat. Res. Soc. (2002) 604.
[13] N. Santander, S.R. Das, S.B. Majumder, R.S. Katiyar, Surf. Coat. Technol. 177–178 (2004) 60.
[14] S.R. Das, I.R. Fachini, S.B. Majumder, R.S. Katiyar, J. Power Sources 158 (2006) 518.
[15] M.M. Thackrey, Y. Shao-Horn, A.J. Kahaian, K.D. Kepler, E. Skinner, J.T. Vaughey, S.A. Hackney, Electrochem. Solid-State Lett. 1 (1998) 7.
[16] H. Huang, C.H. Chen, R.C. Perego, E.M. Kelder, L. Chen, J. Schoonman, W.J. Weydanz, D.W. Nielsen, Solid State Ionics 127 (2000) 31.
[17] H. Huang, C.A. Vincent, P.G. Bruce, J. Electrochem. Soc. 146 (2) (1999) 481.
[18] Y. Shin, A. Manthiram, J. Electrochem. Soc. 151 (2) (2004) A204.
[19] Y. Xia, T. Sakai, T. Fujieda, X.Q. Yang, X. Sun, Z.F. Ma, J. McBreen, M. Yoshio, J. Electrochem. Soc. 148 (7) (2001) A723.
[20] D.S. Ahn, M.Y. Song, J. Electrochem. Soc. 147 (2000) 874.
[21] X.M. He, J.J. Li, Y. Cai, Y. Wang, J. Ying, C. Jiang, C. Wan, J. Solid State Electrochem. 9 (2005) 438.
[22] Y.S. Lee, M. Yoshino, Electrochem. Solid-State Lett. 4 (7) (2001) A85.
[23] S. Nieto, S.B. Majumder, R.S. Katiyar, J. Power Sources 136 (2004) 88.
[24] A.M. Kannan, A. Manthiram, J. Electrochem. Soc. 150 (3) (2003) A349.
[25] J. Molendra, D. Palubiak, J. Marzec, J. Power Sources 144 (2005) 176.
[26] S.J. Bao, W.J. Zhou, Y.Y. Liang, B.L. He, H.L. Li, Mater. Chem. Phys. 95 (2006) 188.
[27] R.E. Melgarejo, M.S. Tomar, S. Bhaskar, P.S. Dobal, R.S. Katiyar, Appl. Phys. Lett. 81 (2002) 2611.
[28] M.S. Tomar, R.E. Melgarejo, A. Hidalgo, S.B. Majumder, R.S. Katiyar, Appl. Phys. Lett. 83 (2003) 341.
[29] S.S. Zhang, K. Xu, T.R. Jow, J. Electrochem. Soc. 149 (12) (2002) A1521.
[30] C.M. Julien, M. Massot, Mater. Sci. Eng. B97 (2003) 217.
[31] Y.K. Sun, K.J. Hong, J. Prakash, J. Electrochem. Soc. 150 (2003) A970.
[32] B. Ammundsen, G.R. Burns, M.S. Islam, H. Kanoh, J. Roziere, J. Phys. Chem. B103 (1999) 5175.